ORIGINAL PAPER

Comparison of Methods for Determining Specific-surface Area of Fine-grained Soils

**D. N. Arnepalli · S. Shanthakumar ·
B. Hanumantha Rao · D. N. Singh**

Abstract Characteristics of fine-grained soils primarily depend on their specific-surface area and hence, reliable determination of this parameter is essential. In this context, researchers have employed quite sophisticated instruments (viz., a BET surface area analyzer, the mercury intrusion porosimetry, internal reflectance spectroscopy, X-Ray diffraction and gas pycnometer etc.) and methodologies (viz., sorption of Methylene Blue dye, Ethylene Glycol Monoethyl Ether and *p*-Nitrophenol) to determine specific-surface area of these soils. However, most of these methodologies are found to be quite tedious, cost and time intensive. Apart from this, the results obtained are contentious due to the inherent limitations associated with either the instruments employed or the basic assumptions made for computing the specific-surface area of the soil. Hence, it becomes mandatory to evaluate the efficiency of these methodologies for determining specific-surface area of fine-grained soils. With this in view, different types of soils were considered in this study and their specific-surface area was determined, by following different methodologies, and the results were evaluated critically. In addition, attempts were made to develop relationships between the basic properties of fine-grained soils (viz., liquid limit, cation-exchange capacity, activity, and free swell index) and the specific-surface area. These relationships will be of immense help to the practicing engineers and research fraternity.

D. N. Arnepalli
Department of Civil Engineering, Queen's
University, Kingston, ON, Canada K7L 3N6
e-mail: naidu@civil.queensu.ca

S. Shanthakumar · B. Hanumantha Rao ·
D. N. Singh (✉)
Department of Civil Engineering, Indian Institute
of Technology Bombay, Powai, Mumbai 400076, India
e-mail: dns@civil.iitb.ac.in

S. Shanthakumar
e-mail: sskumar@iitb.ac.in

B. Hanumantha Rao
e-mail: hanuma_bendadi@iitb.ac.in

Nomenclature

β	a constant parameter
δ	contact angle between the soil and mercury
λ	wavelength of UV-light
ρ_{He}	density of the soil measured with He
ρ_{N_2}	density of the soil measured with N_2
a	absorbance
a_{max}	maximum absorbance
A	activity of the soil

A_{MB}	area covered by each molecule of the Methylene blue (MB) dye	V_a	volume of N_2 adsorbed at pressure P
A_{mol}	area covered by each N_2 molecule	V_{air}	air-adsorption capacity of the soil
A_v	Avogadro's number	V_{Lm}	volume of N_2 required for mono-layer formation as per Langmuir isotherm
b	a parameter	V_{max}	maximum volume of Hg intruded in the sample
C	concentration of the MB dye		
C_e	concentration of the MB dye solution after 24 h	V_{MBET}	volume of N_2 required for mono-layer formation as per multi-point BET isotherm
CEC	cation-exchange capacity	V_{mol}	volume of N_2 molecule
C_i	initial concentration of the MB dye solution	W	weight of the soil
C_{MBET}	a constant	W_c	amount of EMGE absorbed on the sample for mono-layer formation
C_{opt}	optimal amount of the MB absorbed on the soil	W_{EGME}	amount of EGME absorbed on the sample
C_{se}	amount of the MB absorbed on the soil after 24 h	w_{EGME}	amount of EGME required to cover per square meter of Bentonite
C_{si}	amount of the MB, initially added to soil		
G	specific gravity of the soil		
l/s	liquid-solid ratio		
LL	liquid limit of the soil		
MW_{MB}	molecular weight of the MB dye		
p	applied pressure		
P	pressure of N_2 gas		
P/P_0	relative pressure		
P_0	saturation vapor pressure of N_2		
PI	plasticity-index of the soil		
PL	plastic limit of the soil		
S	specific-surface area		
S_{air}	specific-surface area of the soil obtained from air-adsorption method		
S_{ext}	external specific-surface area of the soil		
S_{int}	internal specific-surface area of the soil		
SL	shrinkage limit of the soil		
S_{LM}	specific-surface area of the soil obtained from Langmuir isotherm		
S_{MB}	specific-surface area, obtained from MB absorption technique		
S_{MBET}	specific-surface area, obtained from the multi-point BET isotherm		
S_{MIP}	specific-surface area, obtained from mercury intrusion porosimetry		
FSI	free swell index of the soil		
S_{SBET}	specific-surface area, obtained from the single-point BET isotherm		
S_{total}	total specific-surface area of the soil		
T	surface tension of Hg		
t	time		
V	cumulative volume of mercury intruded into the soil		

1 Introduction

Engineering behavior of most of the fine-grained soils is predominantly influenced by their specific-surface area (Santamarina et al. 2002). Hence, these soils exhibit extremely or relatively high swelling and shrinkage characteristics (Dos and DeCastro 1965; Farrar and Coleman 1967; Ross 1978; Low 1980; Morgenstern and Balasubramanian 1980; Dasog et al. 1988), high frost heave (Nixon 1991), very high collapse and compressibility (Cerato and Lutenegger 2004), high cation-exchange capacity (Mitchell 1993), high water retention characteristics (Warkentin 1972), high activity (Mitchell 1993), and extremely high sorption and desorption characteristics (Daniels et al. 2004). These characteristics mainly depend on the grain-size distribution (i.e., the clay-size fraction) and mineralogical composition (Mitchell 1993) of the soil. However, it has been reported by the researchers that specific-surface area of the soil S alone can capture the combined effect of these factors and hence, can be used for predicting engineering behavior of fine-grained soils (Warkentin 1972; Santamarina et al. 2002). As such, reliable determination of S of fine-grained soils becomes quite essential.

Studies conducted by various researchers for determining S of the fine-grained soils can be grouped as: (a) gas or vapor adsorption techniques such as BET nitrogen adsorption (Brunauer et al. 1938; Tiller and Smith 1990; Santamarina et al. 2002), water-vapor

adsorption technique (Quirk 1955; Orchiston 1959a, b; Newman 1983) (b) absorption of the polar liquids and dyes on the soil surface such as Ethylene glycol (EG) method (Dyal and Hendricks 1950, 1952; Rai and Murari 1963; Mortland and Kemper 1965; Sridharan et al. 1972; Eltantawy and Arnold 1974), Ethylene Glycol Monoethyle Ether (EGME) method (Bower and Goertzen 1959; Tiller and Smith 1990; Carter et al. 1965; Eltantawy and Arnold 1973; Carter et al. 1986; Cerato and Lutenegger 2002), *p*-Nitrophenol method (Ristori et al. 1989; Adamson 1990) and Methylene blue (MB) dye method (Pham and Brindley, 1970; Chen et al. 1999; Santamarina et al. 2002) and (c) application of the state-of-the-art instruments such as mercury intrusion porosimetry (MIP) (Rootare and Prenzlow 1967; Enustun et al. 1990), internal reflectance spectroscopy (Mulla et al. 1985), X-Ray diffraction (Adamson 1990) and gas pycnometer (Tuul and Innes 1962; Allen 1990).

Though most of these methodologies are technically sound, they are quite time-consuming, cost-intensive and require skilled personnel. Apart from this, the results obtained are contentious due to either inherent limitations of the instrument employed or the basic assumptions involved in mathematical models that are used for computing S. Hence, it becomes mandatory to evaluate, critically, the relative efficiency of these methodologies for determining S of a particular soil, and to identify the methodology which is most appropriate, in terms of ease of execution, time and economics.

With this in view, S of fine-grained soils of entirely different types was determined by employing the methodologies cited above, and the results were evaluated critically. In addition, attempts were made to develop relationships between the fundamental engineering characteristics of the fine-grained soils (viz., liquid limit, cation-exchange capacity, activity and free swell index etc.) and S of the soil.

2 Experimental Investigations

2.1 Details of the Materials Used

Locally available silty-soil (designated as ST), clayey silt (CS), black-cotton soil (BC), white clay (WC), Bentonite (BT) and Montmorillonite (MT) were chosen for this study. These soils were characterized for their physical, chemical and mineralogical characterisics by conducting a series of laboratory investigations, details of which are presented in the following.

2.2 Physical Characteristics

The specific gravity G of these soils was determined with the help of an Ultra-Pycnometer (Quantachrome, USA), and the results are presented in Table 1. The particle-size distribution characteristics of these soils were determined following the guidelines provided by ASTM D-422 (ASTM D-422 1994), and the results are presented in Table 2. This table also lists the consistency limits obtained by following the guidelines

Table 1 Details of the soils

Soil	Designation	G
Silt	ST	2.80
Clayey-silt	CS	2.60
Black cotton	BC	2.65
White clay	WC	2.78
Bentonite	BT	2.82
Montmorillonite	MT	2.78

Table 2 Physical characteristics of the soils

Property	Soil					
	ST	CS	BC	WC	BT	MT
Particle size characteristics (%)						
Clay size (<0.002 mm)	25	32	53	54	97	99
Silt size (0.002–0.075 mm)	34	44	27	46	3	1
Sand size (0.075–4.75 mm)	41	24	20	0	0	0
Atterberg limits (%)						
LL	97	61	145	54	227	411
PL	69	37	80	32	92	196
SL	20	18	14	17	15	16
PI	28	24	65	22	135	215
A	1.13	0.75	1.24	0.41	1.39	2.17
FSI (%)[a]	103	33	124	6	179	238
USCS classification	MH	MH	CH	CH	CH	CH

[a] (Thakur and Singh, 2005; Shah, 2005)

Table 3 Chemical composition of the soils

Oxide	% by weight					
	ST	CS	BC	WC	BT	MT
SiO_2	33.59	33.75	47.56	43.46	45.7	56.2
Al_2O_3	9.06	10.87	13.58	33.57	14.04	15.3
Fe_2O_3	14.01	11.77	9.85	1.56	16.28	17.8
TiO_2	1.92	1.76	1.24	3.33	2.42	1.95
CaO	5.31	6.41	3.77	0.37	2.73	3.56
K_2O	0.38	0.65	0.29	0.07	0.37	0.24
MgO	2.44	1.65	1.62	0.74	1.81	1.21
P_2O_5	0.07	0.11	0.04	0.03	0.08	0.06
SrO	0.01	0.02	0.02	0.01	0.03	0.01
MnO	0.21	0.15	0.13	0.05	0.08	0.06
Na_2O	0.68	2.02	0.23	0.17	1.42	1.21
CEC (meq./100 g)	29	19	45	5	38	64

provided by ASTM D-4318 (ASTM D-4318 1994) and ASTM D-427 (ASTM D-427 1994). These soils have also been classified based on the Unified Soil Classification System, USCS (ASTM D-2487 1994), as presented in Table 2. The activity A and free swell index FSI (Thakur and Singh 2005; Shah 2005) of these soils are also presented in the table.

2.3 Chemical and Mineralogical Characteristics

The chemical composition of these soils, in the percentage oxide form, was obtained using an X-Ray fluorescence setup (Phillips 1410, Holland). The cation-exchange capacity CEC of these soils was determined by following the guidelines presented in IS: 2720 (IS 2720 1976) and the results are presented in Table 3.

The mineralogical composition of these soils was determined with the help of an X-Ray diffraction spectrometer (Phillips, Holland), which is fitted with a graphite monochromator and employs Cu-Kα as the source. Minerals present in these soils were identified with the help of JCPDS (JCPDS 1994) search files, as depicted in Table 4.

2.4 Specific-surface Area Determination

Details of methodologies employed for determination of specific-surface area S of the soil sample are presented in the following.

Table 4 Mineralogical composition of the soils

Sample	Minerals present
ST	Albite, Anorthite, Montmorillonite
CS	Anorthite, Quartz, Montmorillonite
BC	Quartz, Mullite
WC	Kaolinite, Illite
BT	Montmorillonite, Illite
MT	Montmorillonite, Kaolinite

2.4.1 Methylene Blue (MB) Absorption Technique

Tests were conducted to determine specific-surface area of the soil sample corresponding to a liquid-solid ratio l/s of 100, and by maintaining the ambient conditions as $27 \pm 0.5°C$ and 50% relative humidity (Pham and Brindley 1970; Santamarina et al. 2002). About 0.5 g of the soil was mixed with 50 ml of MB dye of different initial concentrations ($C_i = 5$ to 10^4 mg/l), in air-tight glass bottles. This mixture was agitated for 24 h by mounting the bottle on a mechanical shaker. Later, the bottle was removed from the shaker and the solution was filtered using the Whatman filter paper. The filtrate was transferred to microfuge tubes and centrifuged at $1,000g$ for 30 min. This process helps in separating soil particles and the solution. The clear solution was decanted, collected in polypropylene tubes and stored in a refrigerator (at 10°C). This process minimizes the precipitation of MB dye and evaporation of the solution. Later, this solution was suitably diluted and analyzed for determining the concentration of MB C_e with the help of a UV-Spectrophotometer (Shimadzu, Japan).

In order to establish the optimum UV-wavelength, at which the MB dye yields maximum absorbance a_{max}, dyes of different concentrations C were tested over a wide range of wavelength ($\lambda = 400$ to 800 nm) and the results are presented in Fig. 1. Attempts were also made to develop a calibration curve (i.e., a relationship between C and a_{max}, at optimal λ value), as depicted in Fig. 2, that can be employed for determining the concentration of the MB dye present in a solution.

2.4.2 Nitrogen (N_2) Gas Adsorption Technique

Tests were conducted to determine specific-surface area of the soil sample using a surface-area analyzer (Autosorb, Quantachrome, USA) with N_2 gas as an
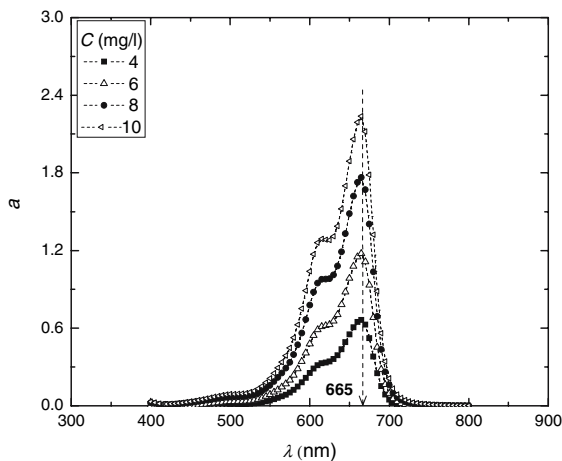
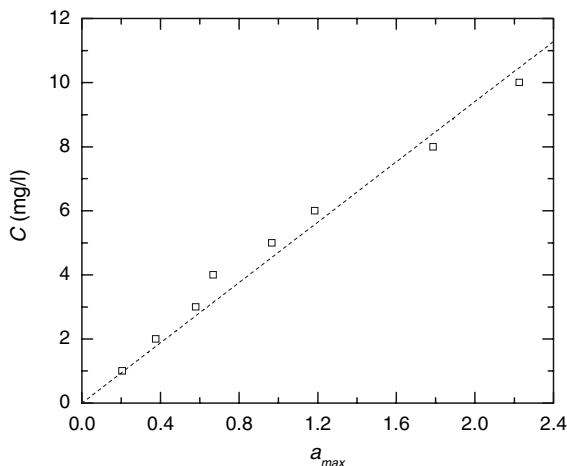**Fig. 1** Absorbance versus wavelength response of MB dye solutions

Fig. 2 Relationship between the maximum absorbance and concentration of the MB dye

adsorbate. This instrument works on BET adsorption theory (Brunauer et al. 1938). For ensuring accuracy of the results, the instrument was calibrated with the help of standard reference material (Alumina) supplied by the manufacturer. Later, 1 g of the air-dried soil sample was poured into a glass-cell and degassed under vacuum at 100°C, for a period of 24 h. This process helps in minimizing errors incurred due to rise of vapor pressure while adsorption of N_2 takes place. The degassing temperature was intentionally maintained very close to the boiling point of water, which ensures no mineralogical alteration during degassing (Zerwer and Santamarina 1994). Later, the sample was exposed to N_2 corresponding to different

relative pressures P/P_0 and maintaining the temperature at 77°K. Where, P and P_0 are pressure and saturation vapor pressures of N_2, respectively. This process ensures optimal adsorption of N_2 (Allen 1990). At the end of the test the sample was weighed on a balance of accuracy 0.0001 g. The volume of N_2 adsorbed V_a on the sample (at pressure P) was recorded and adsorption isotherms were developed, as depicted in Fig. 3.

Further, efforts were made to determine the specific-surface area of the soil by employing a single-point BET analyzer (Smartsorb-91, India). For this purpose, the degassed sample was filled in the sample-holder and it was exposed to N_2. S_{SBET} was obtained with the help of the built-in software, as listed in Table 5.

2.4.3 Ethylene Glycol Monoethyl Ether (EGME) Absorption Method

Specific-surface area of the soil sample was also determined by conducting Ethylene Glycol Monoethyl Ether (EGME) absorption tests (Carter et al. 1986; Cerato and Lutenegger 2002). About 2 g air-dried soil was spread uniformly on the bottom of a glass dish (40 mm in internal diameter and 20 mm in height) and covered with a perforated watch-glass. Six such dishes, with soil sample in them, were placed in a vacuum desiccator containing 250 g of P_2O_5. This helps in maintaining a constant vapor pressure inside the desiccator. The sample was evacuated by applying vacuum for 2 h and was weighed. This process was repeated several times, until sample attains almost a constant weight. Later, 6 ml of analytical grade EGME solution was added to the sample and the mixture was swirled, gently, until it becomes slurry. The slurry was placed in the desiccator over a desiccant (mixture of 100 g $CaCl_2$ and 20 ml EGME) for 12 h. This helps in maintaining a constant vapor pressure and minimizing the loss of EGME from the monolayer, which forms on the surface and the interlayer spacing of the soil minerals. Initial weight of the slurry along with the glass dish was measured, using the precision balance, and the dish was re-placed in the desiccator for evacuation under vacuum. The glass-dish was taken out of the desiccator, weighed and re-placed in it several times, until a constant weight is attained.

Fig. 3 Langmuir and
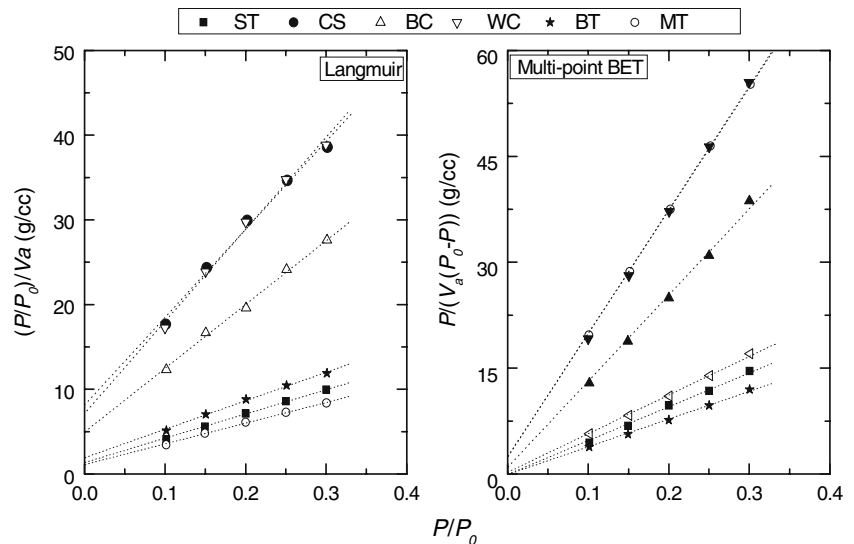multi-point BET adsorption
isotherms for different soils

Table 5 Specific-surface area (in m²/g) of the soils obtained from different methods

Soil	S_{SBET}	S_{MBET}	S_{LM}	S_{MIP}	S_{MB}	S_{EGME}		
						S_{total}	S_{ext}	S_{int}
ST	25.9	74.8	112.8	56.1	243.3	280.6	76.0	204.6
CS	17.7	19.5	33.5	12.9	242.2	127.6	20.5	107.1
BC	37.8	41.2	66.7	28.6	646.6	332.4	42.5	289.9
WC	16.0	19.1	32.1	10.8	64.6	32.0	11.3	20.7
BT	43.5	61.6	102.2	48.2	645.8	352.8	66.7	286.1
MT	54.8	93.3	141	68.6	1057.7	509.8	90.4	419.4

2.4.4 Mercury Intrusion Porosimetry

Mercury Intrusion Porosimetry, MIP, was conducted by employing Poremaster 33™ (Quantachrome, USA), for determining specific-surface area of the soil sample. A known quantity of the air-dried soil was taken in the penetrometer (sample cell) and mounted in the low-pressure port. The penetrometer was evacuated with the help of a vacuum pump which is connected to the instrument. This process helps in degassing the pores of the sample and should be adopted before intruding Hg in it. Later, the sample was weighed along with the penetrometer and was placed back in the low-pressure port. By applying a small pressure, Hg was filled in the penetrometer. Following this, the penetrometer was placed in the high-pressure port and subjected to pressure, in steps, so as to achieve total pressure of 2320 kg/cm². Subsequently, the applied pressure p and

the volume of Hg intruded into the sample V were recorded. After completing this process, the extrusion of Hg from the sample pores was carried out, by reducing the pressure in steps and measuring the extruded volume of Hg corresponding to that pressure. The value of V was corrected for compressibility and temperature, as per the guidelines presented by ASTM D-4404 (ASTM D-4404 1984), by performing blank intrusion test. This was achieved with the help of a non-porous material (i.e., stainless-steel balls of 3 mm diameter).

2.4.5 Air-adsorption Method

Specific-surface area of the soil sample was also measured with the help of a Ultra-pycnometer (Quntachrome, USA). The basic principle of this methodology is that S of the sample is proportional to the air-adsorption capacity V_{air} (Allen 1990; Tuul and Innes 1962). With this in view, V_{air} of the soil sample was determined by measuring the density using Helium ρ_{He} and Nitrogen ρ_{N_2} gases, respectively. The instrument was calibrated using the standard reference material (stainless-steel balls of different diameters) provided by the manufacturer. Later, the air-dried soil sample was degassed at 100°C, under application of vacuum until it attains a constant weight. This procedure ensures complete removal (i.e., desorption) of the adsorbed air from the surface of the sample.

3 Results and Discussion

It can be observed from the results presented in Fig. 1 that, for MB dye the maximum absorbance a_{max}, is attained when λ is equal to 665 nm. This observation is found to be consistent with the results reported in the literature (Santamarina et al. 2002). This ensures proper functioning of the UV-Spectrophotometer and the purity of the MB dye, used in the study.

As depicted in Fig. 2, C versus a_{max} relationship is found to be linear (Eq. 1) and the coefficient of linear regression is 0.9936, which is quite close to unity.

$$C = 4.7 \cdot a_{max} \qquad (1)$$

In addition, blank tests were performed for estimating uptake of MB dye by the glass sampling bottle. The uptake capacity of the sampling bottle, for MB dye, is found to be almost negligible.

Amounts of MB dye initially added to the soil sample (C_{si}, in mg/mg) and that gets adsorbed on the soil particles after 24 h (C_{se}, in mg/mg), were determined using the following relationship.

$$C_{si} = C_i \cdot (l/s) \qquad (2)$$

$$C_{se} = (C_i - C_e) \cdot (l/s) \qquad (3)$$

The C_{se} versus C_{si} plot yields the optimum amount of MB dye (C_{opt}, in mg/mg) that gets adsorbed on the soil sample, as depicted in Fig. 4. It can be noted from the figure that, initially C_{se} increases (depicted as AB) with C_{si} and later it attains a constant value
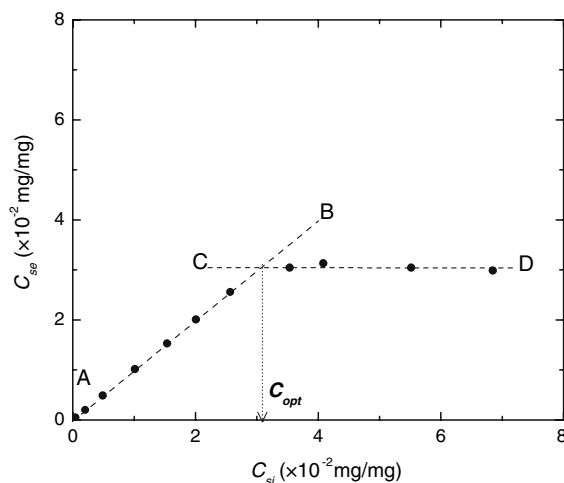

Fig. 4 Determination of optimal concentration of MB dye adsorbed on soil WC

(depicted as CD). The point of intersection of AB and CD yields the optimal amount of the MB dye C_{opt} that gets adsorbed on the soil particles. Hence, C_{opt} corresponds to the state of the soil at which the cations present in the diffused double layer get replaced by the MB dye. As such, C_{opt} can be used for determining the specific-surface area of the soil sample (depicted as S_{MB}) by employing Eq. 4, and results are presented in Table 5.

$$S_{MB} = C_{opt} \cdot \frac{A_v}{MW_{MB}} \cdot A_{MB} \qquad (4)$$

where A_v is Avogadro's number ($=6.02 \times 10^{23}$/mol), A_{MB} is the area covered by each MB molecule ($=13 \times 10^{-19}$ m^2/molecule) and MW_{MB} is the molecular weight of the MB ($=319.87$ g/mol).

Further, N$_2$ adsorption isotherms, represented by Equations 5 and 6 (Santamarina et al. 2002; Brunauer et al. 1938; Langmuir 1918), were developed as depicted in Fig. 3.

$$\frac{P}{P_0 \cdot V_a} = \frac{1}{b \cdot V_{Lm} \cdot P_0} + \frac{P}{P_0 \cdot V_{Lm}} \qquad (5)$$

$$\frac{P}{V_a(P_0 - P)} = \frac{1}{V_{MBET} \cdot C_{MBET}} + \frac{C_{MBET} - 1}{V_{MBET} \cdot C_{MBET}} \cdot \frac{P}{P_0} \qquad (6)$$

where P is the applied pressure, P_0 is the saturation vapor pressure of N$_2$ ($=1$ atm at 77°K), V_a is the volume of N$_2$ adsorbed at P, V_{Lm} is the volume of N$_2$ required for mono-layer formation as per Langmuir isotherm, b is the parameter related to the maximum amount of N$_2$ getting adsorbed on the sample, V_{MBET} is the volume of N$_2$ required to form mono-layer as per multi-point BET isotherm, C_{MBET} is a constant, which is proportional to heat of adsorption in first and subsequent adsorbed layers.

From the slope and intercept on the ordinates of the N$_2$ adsorption isotherms (depicted in Fig. 3) V_{Lm} and V_{MBET} were determined, respectively. Further, using Eq. 7 (Santamarina et al. 2002; Brunauer et al. 1938), specific-surface area (S_{LM} or S_{MBET}) of the sample was computed and the results are presented in Table 5.

$$S_{LM} \text{ or } S_{MBET} = \frac{V_{Lm} \text{ or } V_{MBET}}{V_{mol}} \cdot A_{mol} \qquad (7)$$

where S_{LM} and S_{MBET} are specific-surface areas (in m^2/g) obtained from Langmuir and multi-point BET isotherms, respectively, V_{mol} is the volume of N$_2$

molecule (=1.77×10^{-30} m^3) and A_{mol} is the area covered by each N$_2$ molecule (=16.2×10^{-20} m^2).

The mass in grams of EGME that gets absorbed on a gram of the soil W_{EGME} was computed by subtracting the dry weight of the sample from the weight of the EGME mixed sample. Further, W_{EGME} versus time response for different soils was developed, until it becomes constant. However, for the sake of brevity, only, the response of soil BC is presented in Fig. 5.

Efforts were also made to determine the external surface area S_{ext} of the soil by suppressing the interlayer. For this purpose, the sample was degassed at 600°C for 5 to 6 h under vacuum, prior commencing the EGME test (Carter et al. 1986). Later, S_{ext} of the sample was obtained by following the procedure explained in the previous section and the results obtained are superimposed in Fig. 5. It can be noted from the figure that after a very rapid drop in the weight, the sample attains a constant weight W_c, which corresponds to the formation of monolayer. Hence, the total S_{total} or external S_{ext} specific-surface areas of the soil can be determined by employing Eq. 8 (Carter et al. 1986; Cerato and Lutenegger 2002).

$$S_{total} \text{ or } S_{ext} = \frac{W_c}{w_{EGME}} \tag{8}$$

where w_{EGME} is the amount of EGME required to form monolayer on a square meter of Bentonite (=2.86×10^{-4} g/m^2). The difference between S_{total} and S_{ext} would yield the inter-layer specific-surface area S_{int} of the soil, as presented in Table 5.
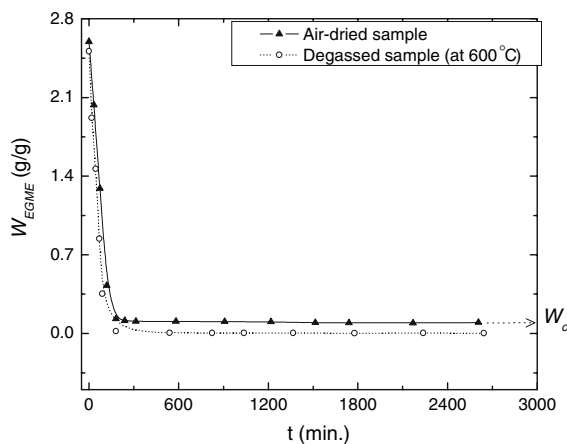
The MIP analysis was conducted on all the soils used in this study. However, for the sake of brevity, results for the soil WC, only, are being presented in Fig. 6. It can be noted from the figure that the cumulative volume of Hg intruded in the soil V increases quite steadily until 35 kg/cm^2 is attained. However, beyond 35 kg/cm^2, V rises quite rapidly until a pressure of 211 kg/cm^2 and beyond which it practically remains constant. Specific-surface area S_{MIP} of the soil can be computed using Eq. 9 (Rootare and Prenzlow 1967; Enustun et al. 1990) and the results are presented in Table 5.

$$S_{MIP} = \int_0^{Vmax} \frac{p \cdot \partial V}{T \cdot \cos \delta} \tag{9}$$

where p is the applied pressure (in kg/cm^2), V_{max} is the maximum volume of Hg intruded in the sample, T is the surface tension of Hg (=0.48 dyne/cm), ∂V is the change in intruded volume of Hg corresponding to a certain incremental pressure and δ is the contact angle (=130°) between the soil and Hg (Enustun et al. 1990).

From the data presented in Table 6 and using Eq. 10 (Allen 1990), V_{air}/W for different soils was determined and the results are presented in Table 6.

$$\frac{V_{air}}{W} = \left[\frac{1}{\rho_{He}} - \frac{1}{\rho_{N_2}} \right] \tag{10}$$

Hence, using V_{air}/W values and Eq. 11 (Allen 1990; Tuul and Innes 1962), the specific-surface area of the soil S_{air} can be obtained.
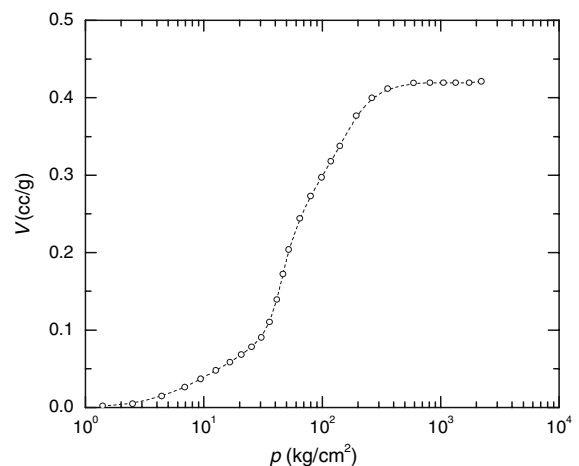

Fig. 5 Variation of W_{EGME} with time for soil BC

Fig. 6 Variation of the volume of mercury intruded with pressure for soil WC

Table 6 Results obtained from air-adsorption method for different soils

Sample	ρ_{He} ($\times 10^6$ g/m^3)	ρ_{N2} ($\times 10^6$ g/m^3)	V_{air}/W ($\times 10^{-8}$ m^3/g)	S_{air} (m^2/g)
ST	2.869	3.636	7.35	68.4
CS	2.772	2.938	2.04	19.0
BC	2.681	2.790	1.45	13.5
WC	2.789	2.960	2.07	19.3
BT	2.821	3.468	6.61	61.5
MT	2.790	3.873	10.03	93.3

$$S_{air} = \frac{\beta V_{air}}{W} \qquad (11)$$

where β is a constant parameter that defines the shape, least dimension and type of the soil particle (Santamarina et al. 2002), and W is the weight of the soil sample.

However, as air-adsorption method involves measurement of the density of the soil in dry state, the inter-layer surface area of the soil may not be accessible to He and N$_2$. Hence, this method will only yield external surface area of the soil (Allen 1990; Tuul and Innes 1962). At the same time, as β influences S of the soil to a great extent, its estimation must be done very accurately.

With this in view, the external surface areas S_{MBET} and S_{EGME} of different soils, obtained from MBET and EGME methods, respectively, were correlated with V_{air}/W, as depicted in Fig. 7. It can be observed
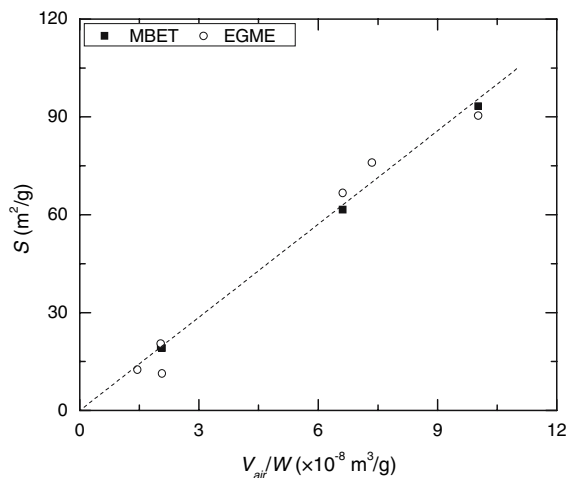

Fig. 7 Estimation of β using MBET and EGME results

from the figure that the variation of V_{air}/W with S_{MBET} and S_{EGME} is linear and the coefficient of regression is almost unity (=0.9926). This relationship yields β equal to 943×10^6 m^{-1}, which can be used for estimating the specific-surface area S_{air} of different soils (Eq. 11), as listed in Table 6.

It can be noticed from the data presented in Tables 5 and 6 that N$_2$ adsorption (i.e., single-point BET, multi-point BET and Langmuir isotherm), air-adsorption (i.e., pycnometer) and mercury intrusion porosimetry techniques yield quite low specific-surface areas as compared to their counter parts (i.e., EGME and MB methods). This can be attributed to the fact that due to the dry state of the sample employed by these three methods, the inter-layer of the soil gets suppressed. Hence, the difference between the value of S for a soil, under dry and wet conditions would be more, particularly, for expansive soils (Carter et al. 1986). The difference between these two S values can also be attributed to the fact that the active absorption sites available for weakly adsorbed molecules (N$_2$ and He) are quite less. This is mainly due to the reduction in accessible inter-layer surface area of the clay minerals present in the soil (Santamarina et al. 2002; Daniels et al. 2004; Carter et al., 1986).

It can also be noted that, in general, the value of S obtained from Langmuir isotherm S_{LM} is quite high as compared to the value obtained from the multi-point BET technique S_{MBET}. This can be attributed to the basic assumption associated with the Langmuir isotherm that only mono-layer formation occurs with N$_2$ adsorption (Langmuir 1918). However, in reality adsorption of molecules on the surface of the soil particle takes place in the form of multi-layers and hence the multi-point BET would yield more generalized results (Brunauer et al. 1938).

As depicted in Table 5, the single-point BET method yields lesser value of specific-surface area S_{SBET} as compared to the value obtained from the multi-point BET test S_{MBET}. This can be attributed to the fact that single-point BET response i.e., volume of N$_2$ adsorbed by a material over a wide range of the relative pressure is linear (Brunauer et al. 1938).

Hence, it can be concluded that the methods that employ dry state of soils (i.e., N$_2$ adsorption, mercury intrusion porosimetry and air-adsorption) for determination of the specific-surface area may not yield accurate results due to non accessibility

of the inter-layer surface for adsorption of molecules (Santamarina et al. 2002). At the same time, these methods fail to explain the effect of soil-water interaction on specific-surface area of a material. In contrast, MB and EGME methods involve wet state of the soil and hence yield total specific-surface area, which in real sense governs engineering behavior of the soil. In general, MB method yields higher value of the specific-surface area S_{MB} as compared to S_{total} obtained from the EGME method. This can be attributed to the basic assumption that the MB molecule, which is prismoidal in shape, gets adsorbed on the soil surface in such a way that the largest dimension is in-plane with the surface. In this orientation, each molecule of MB covers approximately 130 $\mathring{A}^2$ of the soil surface. As such, MB method over predicts the specific-surface area of the fine-grained soils (Chen et al. 1999; Santamarina et al. 2002).

It can also be observed from the data presented in Table 5 that S_{ext} of different soils obtained from EGME method matches very well with S_{MBET}. This demonstrates that EGME method of determining specific-surface area of soils is the most reliable method out of so many methods being adopted by the researchers. At the same time, EGME method yields results quite rapidly and without being much expensive.

3.1 Determination of Characteristics of Fine-grained Soils Using Specific-surface Area

Further, efforts were made to develop generalized relationships between basic characteristics of fine-grained soils (such as liquid limit LL, cation-exchange capacity CEC, activity A and free swell index FSI) and their specific-surface area ($S = S_{total}$), by plotting results, of approximately 70 soils, available in literature (Farrar and Coleman 1967; Low 1980; Erdal 2002; Cerato and Lutenegger 2002; Dolinar and Trauner 2004), as depicted in Figs. 8–11. These parameters imbibe physical, chemical, mineralogical and geotechnical characteristics of a soil. It should also be appreciated that S_{total} obtained from EGME method yields most reliable specific-surface area for a fine-grained soil. The trends depicted in Figs. 8–11 can be represented as:

$$LL = 0.1 \cdot (S_{total})^{1.33} \tag{12a}$$

$$CEC = 0.13 \cdot S_{total} \tag{12b}$$

$$A = 0.5 + (1 \times 10^{-4} \cdot (S_{total})^{1.5}) \tag{12c}$$

$$FSI = 0.42 \cdot S_{total} \tag{12d}$$

Further, results of the six soils (ST, CS, BC, WC, BT and MT) used in this study were superimposed on Figs. 8–11 and an excellent matching of the results with the trends can be noted. This indicates that the developed relationships are quite general in nature
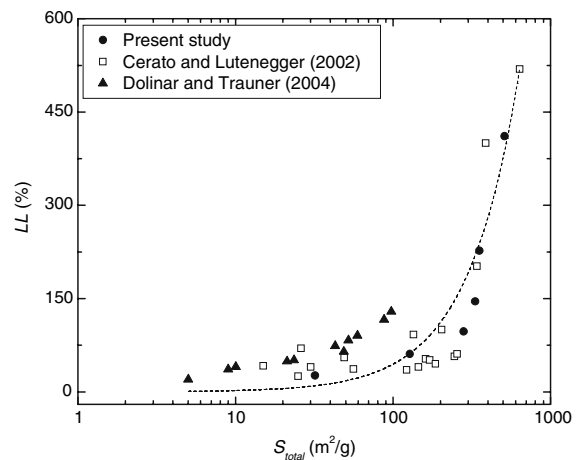

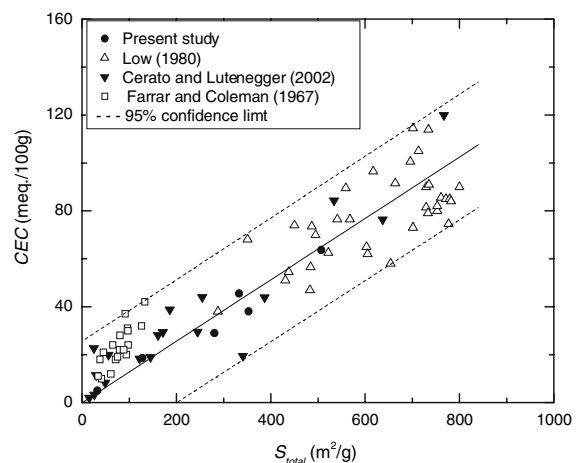**Fig. 8** Relationship between specific-surface area and liquid limit of the soil

Fig. 9 Relationship between specific-surface area and cation-exchange capacity of the soil
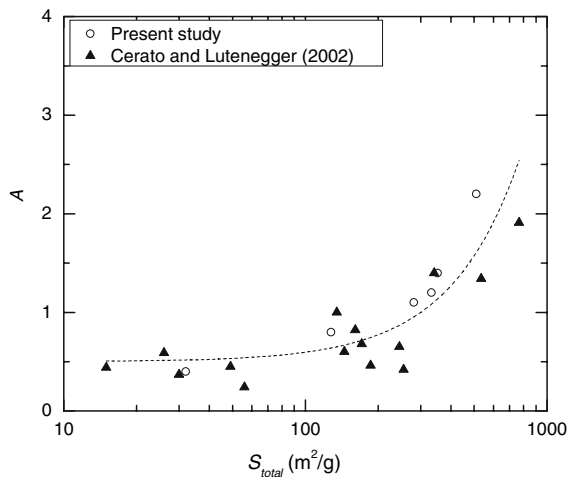
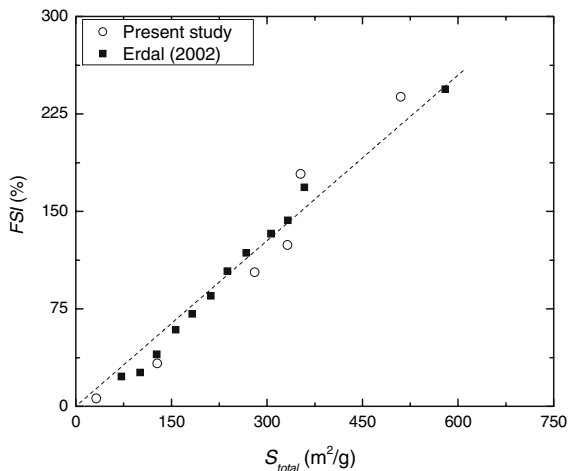**Fig. 10** Relationship between specific-surface area and activity of the soil

Fig. 11 Relationship between specific-surface area and FSI of the soil

and can be used for reliable estimation of *LL*, *CEC*, *A* and *FSI* of fine-grained soils by inputting their specific-surface area.

4 Concluding Remarks

The study brings out a simple methodology that can be used for determination of specific-surface area of the fine-grained soils, based on a critical evaluation of various methodologies that are being adopted by the researchers, presently. It has been demonstrated that EGME method yields most reliable results and at the

same time is quite economical in terms of time and cost. It has also been shown that empirical relationships between basic characteristics of fine-grained soils (such as liquid limit, cation-exchange capacity, activity and free swell index) and the specific-surface area are quite generalized in nature. Hence, for fine-grained soils these characteristics can be estimated, reliably, just by knowing their specific-surface area.

References

Adamson AW (1990) Physical chemistry of surfaces. John Wiley & Sons, New York

Allen T (1990) Particle size measurement. Chapman and Hall, New York

ASTM D-2487 (1994) Standard test method for classification of soils for engineering purposes (unified soil classification system), *Annual Book of ASTM Standards*, 04.08, ASTM International, West Conshohocken, PA, USA, pp 206–215

ASTM D-422 (1994) Standard test method for particle size analysis of soils. *Annual Book of ASTM Standards*, 04.08, ASTM International, West Conshohocken, PA, USA, pp 10–16

ASTM D-427 (1994) Standard test method for shrinkage factors of soils by the mercury method. *Annual Book of ASTM Standards*, 04.08, ASTM International, West Conshohocken, PA, USA, pp 21–24

ASTM D-4318 (1994) Standard test method for liquid limit, plastic limit and plasticity index of soils. *Annual Book of ASTM Standards*, 04.08, ASTM International, West Conshohocken, PA, USA, pp 551–561

ASTM D-4404 (1984) Standard test method for determination of pore volume and pore volume distribution of soil and rock by mercury intrusion porosimetry, *Annual Book of ASTM Standards*, 12.01, ASTM International, West Conshohocken, PA, USA, pp 1–5

Bower CA, Goertzen JO (1959) Surface area of soils and clays by an equilibrium ethylene glycol method. Soil Science 87:289–292

Brunauer S, Emmett PH, Teller E (1938) Adsorption of gases in multi-molecular layers. J Am Chem Soc 60:309–319

Carter DL, Heilman MD, Gonzalez CL (1965) Ethylene glycol mono-ethyl ether for determining surface area of silicate minerals. Soil Sci 100(5):356–360

Carter DL, Mortland MM, Kemper WD (1986) Specific surface, methods of soil analysis. American Society of Agronomy, USA

Cerato AB, Lutenegger AJ (2002) Determination of surface area of fine-grained soils by the ethylene glycol mono-ethyl ether (EGME) method. Geotech Testing J 25(3):1–7

Cerato AB, Lutenegger AJ (2004) Determining intrinsic compressibility of fine-grained soils. Journal of Geotechnical and Geoenvironmental Engineering 130(8):872–877

Chen G, Pan J, Han B, Yan H (1999) Adsorption of methylene blue on montmorillonite. J Dispersion Sci Technol 20(4):179–1187

Daniels JL, Inyanh HI, Brochu Jr M (2004) Specific surface area of barrier mixtures at various outgas temperature. J Environ Eng 130(8):867–872

Dasog GS, Acton DF, Mermut AR, DeJong E (1988) Shrink-swell potential and cracking in clay soils of Saskatchewan. Can J Soil Sci 68:251–260

Dolinar B, Trauner L (2004) Liquid limit and specific surface of clay particles. Geotech Testing J 27(6):580–584

Dos SMPP, DeCastro E (1965) Soil erosion in roads. Proc 6th Int Conf Soil Mech Foundation Eng 1:116–118

Dyal RS, Hendricks SB (1950) Total surface area of clays in polar liquids as a characteristic index. Soil Sci 69:421–432

Dyal RS, Hendricks SB (1952) Formation of mixed layer minerals by potassium fixation in montmorillonite. Soil Sci Soc Am Proc 16:45–48

Eltantawy IM, Arnold PW (1973) Reappraisal of ethylene glycol mono-ethyl ether (EGME) method for surface area estimations of clays. J Soil Sci 24:232–238

Eltantawy IM, Arnold PW (1974) Ethylene glycol sorption by homoionic montmorillonites. J Soil Sci 25:99–110

Enustun BV, Gunnink BW, Demirel T (1990) Phase transition porosimetry and surface area determination. J Colloid Interf Sci 134(1):264–274

Erdal C (2002) Relationship between methylene blue value, initial soil suction and swelling percent of expansive soils. J Eng Environ Sci 26:521–529

Farrar DM, Coleman JD (1967) The correlation of surface area with other properties of nineteen British clay soils. J Soil Sci 18(1):118–124

IS 2720 Part XXIV (1976) Methods of test for soils determination of cation exchange capacity. Indian Standards Institute, New Delhi, India

JCPDS, Powder Diffraction File 44 7354-CD ROM (1994), International Centre for Diffraction Data. Pennsylvania, USA

Langmuir I (1918) The adsorption of gases on plane surfaces of glass, mica and platinum, J Am Chem Soc 40:1361–1402

Low PF (1980) The swelling of clay: II. Montmorillonite, Soil Sci Soc Am J 44(4):667–676

Mitchell JK (1993) Fundamentals of soil behavior. John Wiley & Sons, New York

Morgenstern NR, Balasubramanian BI (1980) Effects of pore fluid on the swelling of clay-shale. Proc 4th Int Conf Expansive Soils 1:190–205

Mortland MM, Kemper WD (1965) Specific surface, methods of soil analysis. American Society of Agronomy, USA

Mulla DJ, Low PF, Roth CB (1985) Measurement of the specific surface area of clays by internal reflectance spectroscopy. Clays Clay Minerals 33(5):391–396

Newman ACD (1983) The specific surface of soils determined by water sorption. J Soil Sci 34:23–32

Nixon JF (1991) Discrete ice lens theory for frost heave in soils. Can Geotech J 28:843–859

Orchiston HD (1959) Adsorption of water vapor: VI. ca-soils at 258°K. Soil Sci 87:350–352

Orchiston HD (1959) Adsorption of water vapor: VII. allophane and some clay materials at 258 °K, Soil Sci 88:159–163

Hang PT, Brindley GW (1970) Methylene blue absorption by clay minerals: determination of surface areas and cation exchange capacities. Clays Clay Minerals 18:203–212

Quirk JP (1955) Significance of surface areas calculated from water vapor sorption isotherms by use of the BET equation. Soil Science 80:423–430

Rai PB, Murari K (1963) Studies in surface area measurements of soils: I comparison of different methods. Soil Sci 96:331–335

Ristori GG, Sparvoli E, Landi L, Martelloni C (1989) Measurement of specific surface areas of soils by p-nitrophenol adsorption. Appl Clay Sci 4:521–532

Rootare HM, Prenzlow CF (1967) Surface area from mercury porosimeter measurements. J Phys Chem 71(8):2733–2736

Ross GJ (1978) Relationships of specific surface area and clay content to shrink-swell potential of soils having different clay mineralogic compositions. Can J Soil Sci 58:159–166

Santamarina JC, Klein KA, Wang YH, Prencke E (2002) Specific surface area: determination and relevance. Can Geotech J 39:233–241

Shah PH (2005) Some Studies on Electrical Properties of Soils, Ph.D. Thesis, Submitted to Department of Civil Engineering, IIT Bombay, India

Sridharan A, Rao G, Venkatappa R (1972) Surface area determination of clays. Geotech Eng 3:127–132

Thakur VKS, Singh DN (2005) Rapid Determination of swelling pressure of clay minerals. J Testing Eval ASTM 33(4):1–7

Tiller KG, Smith LH (1990) Limitations of EGME retention to estimate surface area of soils. Aust J Soil Sci 28:1–26

Tuul J, Innes WB (1962) Inorganic oxide air adsorption at room temperature and correlation with surface area. Anal Chem 36(7):818–820

Warkentin BP (1972) Use of the liquid limit in characterizing the clay soils. Can J of Soil Sci 52:457–464

Zerwer A, Santamarina JC (1994) Double layers in pyro-metamorphosed bentonite: index properties and complex permittivity. Appl Clay Sci 9:283–291